



Skeletal Structures for Modeling Generalized Chamfers and Fillets in the Presence of Complex Miters

Martin Held¹ , Peter Palfrader² 

¹FB Computerwissenschaften, University of Salzburg, Austria, held@cs.sbg.ac.at

²FB Computerwissenschaften, University of Salzburg, Austria, palfrader@cs.sbg.ac.at

Corresponding author: Martin Held, held@cs.sbg.ac.at

Abstract. A chamfer is a sloped or angled corner or edge that provides a transition between faces of a three-dimensional object. Similarly, a fillet is a rounded corner or edge. We show how to model and construct complex chamfers and fillets for extruded objects in a robust and efficient way even if several faces of the object are involved. Our approach is based on skeletal structures such as the medial axis and straight skeleton of the footprint of the extruded object. It can be seen as a generalization of the standard roofs induced by these structures.

Keywords: Roof, Chamfer, Fillet, Voronoi diagram, Straight Skeleton

DOI: <https://doi.org/10.14733/cadaps.2019.620-627>

1 INTRODUCTION

A chamfer is a sloping surface or edge that provides a transition between two faces of an object. A symmetrical chamfer is obtained if the original elements are trimmed by an equal amount. Similarly, a fillet is the rounding-off of an edge. Chamfers and fillets may be formed among either inside or outside adjoining faces of an object. The geometry of a fillet is given by the graph of a concave function, when applied to an interior corner or edge, and the graph of a convex function when on an outside corner or edge.

Both chamfers and fillets are widely applied in manufacturing as well as in other disciplines, e.g., in architecture. Their use ranges from easing otherwise sharp edges, both for safety reasons and to prevent damage to them, to modeling welds and material inaccessible to (and unremovable by) machine tools, and ends in purely aesthetic applications. The complexity of these features varies greatly depending on the application.

We note that the terminology regarding chamfers and fillets does not seem to be established consistently and rigidly. For instance, fillets applied to outside corners or edges tend also to be referred to as “rounds”. And in the machining industry the terms “chamfer” and “bevel” often seem to be used interchangeably.

We content ourselves with an intuitive understanding of these concepts and focus on their modeling in the presence of complex interactions between various faces around a “corner” or “edge”. Complex chamfers may occur, for instance, at the corners of frames for paintings and heraldic signs. In architecture, modern designs of roofs of sport arenas (like soccer stadiums or outdoor climbing facilities) result in curved or cross-gabled patches over multi-corner buildings which can be seen and modeled as complex generalized chamfers. Complex fillets may occur at the corners of pockets when a roundnose tool or bullnose tool is lifted upwards while being driven towards the corners of the pocket.

1.1 Our contribution

In this paper we study the generation of complex chamfers and fillets at the corners of solid objects generated by extruding a two-dimensional (polygonal) shape. The underlying mathematical concept that drives our work is given by the theory of skeletal structures, such as the medial axis and its straight-line relative, the straight skeleton. In a nutshell, these skeletal structures partition the plane into regions such that all points of one region are closer to one input entity than to all other input entities. The precise meaning of “closer” and “input entity” depends on the specific skeletal structure. For an input polygon P in the plane \mathbb{R}^2 , both structures can be constructed by wavefront propagation, where an offsetting process causes P to shrink while obeying certain rules. During the offsetting process, an offset structure traces out the interior of P , arriving at each locus with coordinates (x, y) at a specific point in time $t(x, y)$. By interpreting t as z -coordinate one obtains points in \mathbb{R}^3 with coordinates (x, y, t) . The set of all these points forms a three dimensional structure which is commonly called the roof of P .

We extend this standard roof interpretation by a conceptually simple yet powerful method which allows modeling various styles of roofs or sinks. Basically, we still lift the area bounded by P into \mathbb{R}^3 but we generalize how the z -coordinate for each point of the roof-like surface is obtained. We can handle arbitrary polygonal areas with and without holes, and one method also supports boundary curves that consist of circular arcs in addition to straight-line segments.

The possibility to play with different functions for this lifting from \mathbb{R}^2 to \mathbb{R}^3 allows to create a comprehensive family of roof-like surfaces for one particular input and corresponding skeletal structure. Hence, this new approach provides a genuine extension of the roofs discussed in our prior work [13], where the shape and geometry of a roof is fixed once the skeletal structure has been fixed.

Of course, standard CAD systems offer functionality for chamfering and filleting for the setting described above. However, we are not aware of prior publications that put these operations on a solid theoretical basis. In any case, we note that the use of skeletal structures makes it possible to obtain these roof-like surfaces without a need for brute-force computations in order to compute interactions among the facets of the surface.

2 VORONOI DIAGRAM

Consider a finite set S of points in the Euclidean plane. The area that is closer to a point $p \in S$ than to any other point of S is called that point's *Voronoi region*, and p is called the defining *site* of that Voronoi region. Each Voronoi region belongs to exactly one site. The boundary of a Voronoi cell is formed by *Voronoi edges*, and the points shared by three or more Voronoi edges are called *Voronoi nodes*. The *Voronoi diagram* is given by the union of the Voronoi edges; see Figure 1(a) for the Voronoi diagram (clipped to a finite portion of the plane) of a set of 16 point sites (green). Every Voronoi edge lies on the *bisector* of its two defining sites, i.e., on the set of points equidistant to both sites.

This concept can be illustrated by the prairie-fire analogy [5]: Suppose that fires start in all points of S at the same time, spreading out uniformly in all directions at unit speed. A point in the plane then belongs to the region of the site whose fire reached it first. The loci where two fire waves meet make up the edges of the Voronoi diagram.

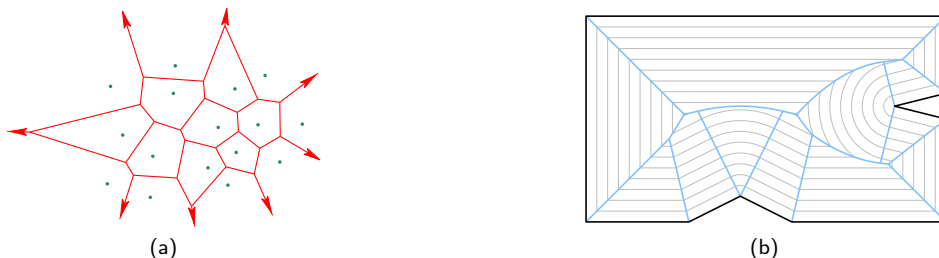


Figure 1: (a) The Voronoi diagram (red) of 16 point sites (green). (b) The Voronoi-diagram (blue) of an input polygon P (black) with wavefronts (gray) at different times during the propagation process.

The same approach can be used not just for points, but also for more general input sets like a polygon P , with the edges and vertices of P forming the set of sites. Figure 1(b) shows this propagation at different times together

with the resulting Voronoi diagram. At time $t := 0$ all edges and vertices of P emanate a wave which moves towards the interior of P with unit speed. Initially, at time $t = \varepsilon$, the wavefront will consist of line segments, stemming from the edges of the polygon, and circular arc segments, stemming from the reflex vertices of P . (As usual, a vertex of a polygon P is called “reflex” if the interior angle at p is greater than 180° .) As the wavefront propagates, the wavefront will undergo changes as segments will shrink to zero length and get dropped, or when the wavefront splits into parts when different parts of the wavefront meet. Figure 1(b) shows the wavefront at different times during this propagation process.

Once all wavefront segments have collapsed and vanished, the wavefront propagation has finished. The edges of the Voronoi diagram then comprise the traces of the vertices of the wavefront over the propagation time. In Figure 1(b), the resulting Voronoi diagram is depicted in blue. We note that a Voronoi diagram will contain edges that are parabolic arcs if it contains reflex vertices. This concept can be generalized further by allowing the waves to propagate also to the exterior of P , or by replacing P by an arbitrary collection of straight-line segments and circular arcs that do not intersect pairwise except for (possibly) sharing common endpoints.

Voronoi diagrams of n points, straight-line segments and circular arcs can be computed efficiently in $\mathcal{O}(n \log n)$ time, both in the worst case [8, 19] and in the expected case [10, 12]. For one simple polygon with n vertices even a linear-time deterministic solution is known [6]. We refer to Held [11] for more information on the theory and application of Voronoi diagrams. For this work we used the VRONI/ARCVRONI package described in [10, 12].

3 STRAIGHT SKELETON

The concept of straight skeletons was first mentioned in the 19th century by Peschka [16], and was re-introduced to computational geometry two decades ago by Aichholzer et al. [1]. The straight skeleton of a polygon P is defined as the result of a wavefront propagation process similar to that used to illustrate the Voronoi diagram. The main difference is that a reflex vertex v of P does not emanate a circular arc. Instead, the wavefront edges emanated from the edges incident at v move inwards with their common wavefront vertex moving towards the interior of P on their angular bisector. Figure 2(a) demonstrates this property. As in Voronoi diagrams, the edges of the straight skeleton are the traces of the wavefront vertices, and the straight skeleton tessellates the interior of P into faces with exactly one face per input edge. However, as its name suggests and in contrast to Voronoi diagrams, all its edges are formed by straight-line segments.

Straight skeletons are linked intrinsically with roofs [1]. Regard the edges of a polygon P as the exterior footprint (i.e., bird’s eye view) of a building and construct a roof such that water drains to the outside and such that all facets of the roof have the same inclination, with exactly one facet per edge of P . Projecting this unique roof to the two-dimensional xy -plane will result in the straight skeleton of P : The roof facets project to straight skeleton faces, and the ridges and valleys in the roof project to the edges of the straight skeleton.

It is well known that mitered offset intersections for acute angles at reflex vertices can be far away from their defining input. To remedy this problem, straight skeletons can be generalized by also sending out wavefront segments at reflex vertices of P , thus obtaining a so-called *linear axis* [17]. Then wavefronts correspond to beveled offsets where the distance between any offset curve point and its input is bounded by c times the orthogonal offset distance, for some user-specified constant c . See Figure 2(b) for a sample linear axis and the corresponding wavefronts. Further generalizations include replacing a polygon as input for a straight-skeleton algorithm by an arbitrary collection of straight-line segments that do not intersect except at common endpoints. Furthermore, one can assign both additive and multiplicative weights to the edges, causing some wavefront edges to move at a higher speed or to start moving at a later time than other edges.

From a theoretical point of view the currently best algorithm for computing the straight skeleton of an arbitrary simple polygon with n vertices is due to Eppstein and Erickson [7]; it runs in $\mathcal{O}(n^{17/11+\epsilon})$ worst-case time and space, for any $\epsilon > 0$. The algorithm by Vigneron and Yan [18] achieves an expected $\mathcal{O}(n^{4/3} \log n)$ time complexity but is only applicable if no so-called multi-split events occur. Biedl et al. [3] investigate multiplicatively-weighted straight skeletons.

Practically efficient algorithms are due to Held, Huber and Palfrader [14, 15]. An easy-to-implement algorithm by Biedl et al. [2] allows to compute the straight skeleton of a monotone polygon with n vertices in $\mathcal{O}(n \log n)$ time. For this work we used Palfrader’s SURFER code [15] to construct (weighted) straight skeletons.

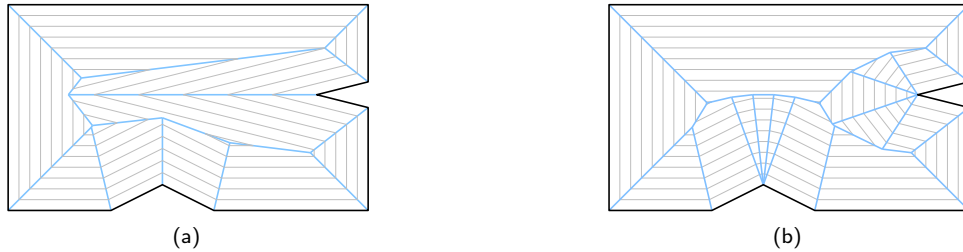


Figure 2: (a) The straight skeleton (blue) of the same polygon. (b) A linear axis results from beveling at reflex vertices of the polygon.

4 GENERALIZED ROOFS FOR MODELING COMPLEX CHAMFERS

In the previous section we mentioned that the straight skeleton of P can be obtained by projecting the unique roof of a building with walls P to the xy -plane. The reverse process, i.e., obtaining the roof from the straight skeleton, is also possible: Suppose that P lies in the xy -plane of \mathbb{R}^3 and let $\mathcal{W}_P(t)$ be the wavefront of P at time t . Consider all wavefronts over the propagation period and raise each wavefront in the z -coordinate by its time t . This will result in a piecewise-linear and continuous surface $\mathcal{R}(P) := \bigcup_{t \geq 0} (\mathcal{W}_P(t) \times \{t\})$, the roof of P ; see Figure 3(b). By construction, this surface is monotone relative to the xy -plane, i.e., every line parallel to the z -axis intersects it in at most one point. The z -isolines of this surface at height t are formed by $\mathcal{W}_P(t) \times \{t\}$.

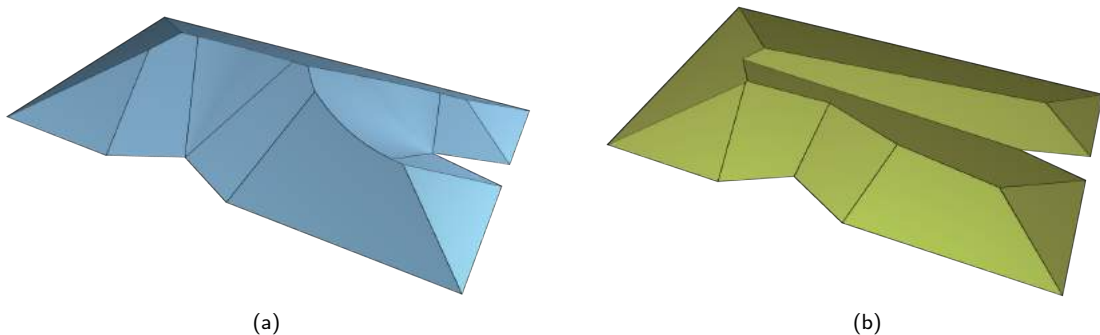


Figure 3: The roofs induced by the Voronoi diagram (a) and the straight skeleton (b) of the polygon shown in Figures 1(b) and 2(a).

The same construction principle can also be applied to a wavefront that traced out a Voronoi diagram. Again one gets a continuous surface; see Figure 3(a). However, such a roof is no longer necessarily piecewise-linear since it may contain facets formed by ruled surfaces. As discussed in the previous sections, the actual meaning of the boundary distance t changes in the neighborhood of reflex vertices when basing the construction on a Voronoi diagram rather than on a straight skeleton.

Since there is no stringent theoretical need to use the boundary distance t as z -coordinate for a point on $\mathcal{W}_P(t)$, we can generalize this construction scheme by replacing t by some height function $f: \mathbb{R}_0^+ \rightarrow \mathbb{R}$ of t , which maps every non-negative argument t to a height value. Of course, it is fine to define f only over the interval $[0, t_{max}]$ rather than over all of \mathbb{R}_0^+ if t_{max} is the maximum value of t for which $\mathcal{W}_P(t)$ does not vanish.

We use a (continuous) height function f to obtain a scalar field on P , thereby generalizing the roof $\mathcal{R}(P)$ to a surface $\mathcal{T}_f(P): \mathcal{T}_f(P) := \bigcup_{t \geq 0} (\mathcal{W}_P(t) \times \{f(t)\})$. By construction, the normal projection of a contour line of $\mathcal{T}_f(P)$ with z -coordinate t onto P equals $\mathcal{W}_P(t)$. Also by construction, $\mathcal{T}_f(P)$ is monotone relative to the xy -plane. Due to its resemblance to an elevation model of an actual landscape over P we refer to $\mathcal{T}_f(P)$ as *terrain* over P .

For Voronoi-based wavefronts $\mathcal{W}_P(t)$ we can visualize this terrain generated by using $f(t)$ as z -coordinates as

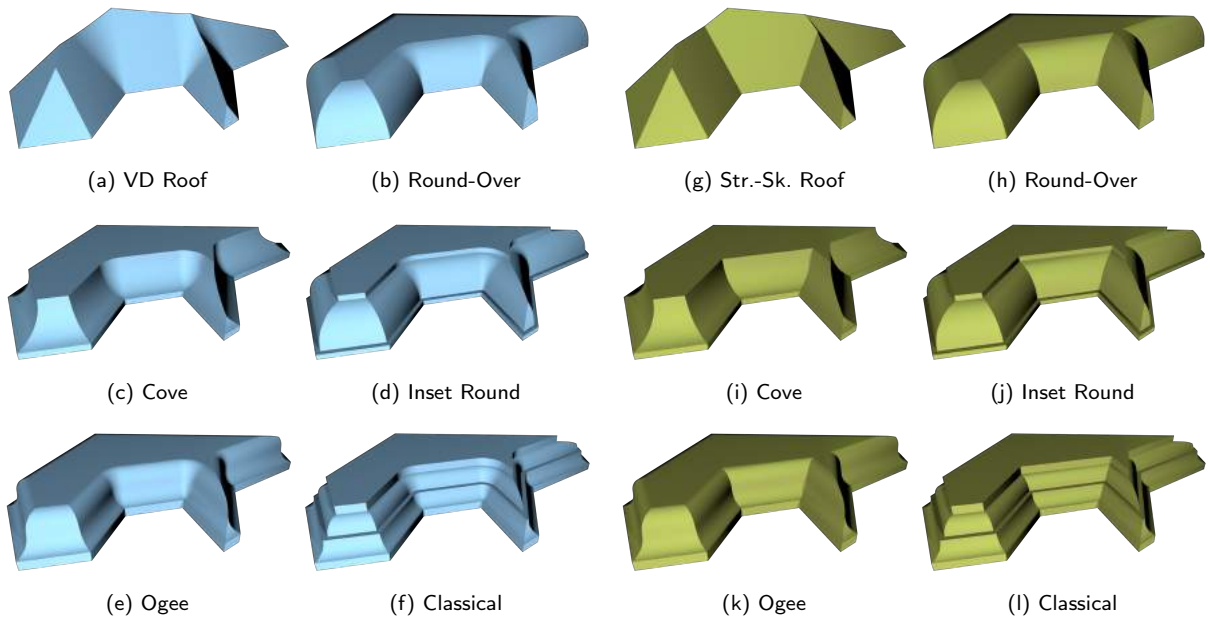


Figure 4: A sample collection of chamfers based on a Voronoi diagram (left, blue) and mitered chamfers based on a straight skeleton (right, olive-green). (Visit Held's CGA Lab [9] for larger images and several other examples.)

follows: Imagine that a solid object is formed by extruding the polygon P along the z -axis. By rotating the height function f around the z -axis we obtain a surface of revolution SR . We now drive an imaginary router bit whose boundary surface matches SR along P such that the tip of the tool follows the boundary of P and such that its axis of rotation stays parallel to the z -axis. Driving that tool along P in the manner described results in a sculpting operation which creates a surface that is identical to the terrain $\mathcal{T}_f(P)$. We note that this interpretation does not hold for mitered wavefronts: The router bit would not be able to machine the valleys that originate at reflex vertices of P .

From a theoretical point of view, the height function f is not required to be continuous. If, however, f is a piecewise continuous function then $\mathcal{T}_f(P)$ will be piecewise continuous, too, and lower and higher portions of the roof will be separated by vertical "walls". Similarly, f is not required to be monotonically increasing. If f is monotonically decreasing then the terrain $\mathcal{T}_f(P)$ does not model a "mountain range" that rises from P but some "underwater landscape". If f is neither monotonically increasing nor monotonically decreasing then the resulting terrain will contain ditches that wind around peaks like moats used to wind around medieval castles, or rims and ridges that bound areas at lower z -levels, like a crater lake within a volcano.

A collection of sample terrains is shown in Figure 4. Note that Figure 4(a) shows the standard Voronoi-diagram induced roof, $\mathcal{R}(P)$, and Figure 4(g) shows the standard straight-skeleton roof. See Figure 5(a) for the specific height function used for obtaining the surfaces shown in Figures 4(f) and 4(l). A chamfering of the outline of an island and chamfers of a polygon with holes are shown in Figure 6.

If a facet of this terrain is incident to a boundary edge e of P then it constitutes a ruled surface. In particular, all facets of a terrain obtained from a straight skeleton are ruled surfaces. The facet incident at e is defined by sweeping a line such that it passes through one point on its left ridge or valley and through one point on its right ridge/valley. During the entire sweeping process the line stays parallel to e . If the terrain was obtained from a Voronoi diagram then all facets incident at reflex vertices are surfaces of revolution, i.e., portions of the surface SR of the router bit.

Of course, it depends on the mathematical nature of the height function f whether or not it is feasible to model the facets of such a terrain analytically. Most definitely, an exact analytical modeling is possible if f is a piecewise-linear function since then also $\mathcal{T}_f(P)$ is piecewise-linear and, thus, at least in this case it is fairly easy to model the facets of $\mathcal{T}_f(P)$ analytically.

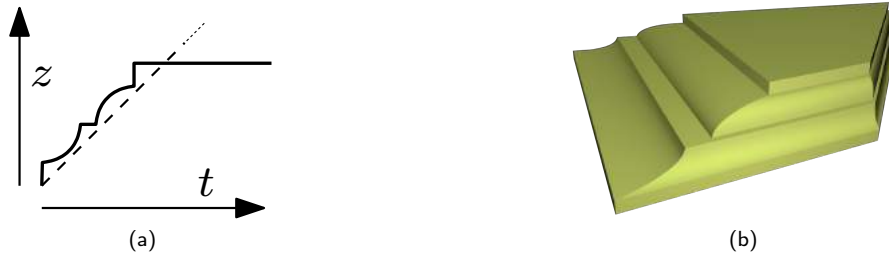


Figure 5: (a) The height function used for obtaining the surfaces shown in Figures 4(f) and 4(l). The standard height function which results in the roofs of Figures 4(a) and 4(g) is shown by a dashed line. (b) Mitered chamfers based on a multiplicatively weighted straight skeleton also using the height function from (a).

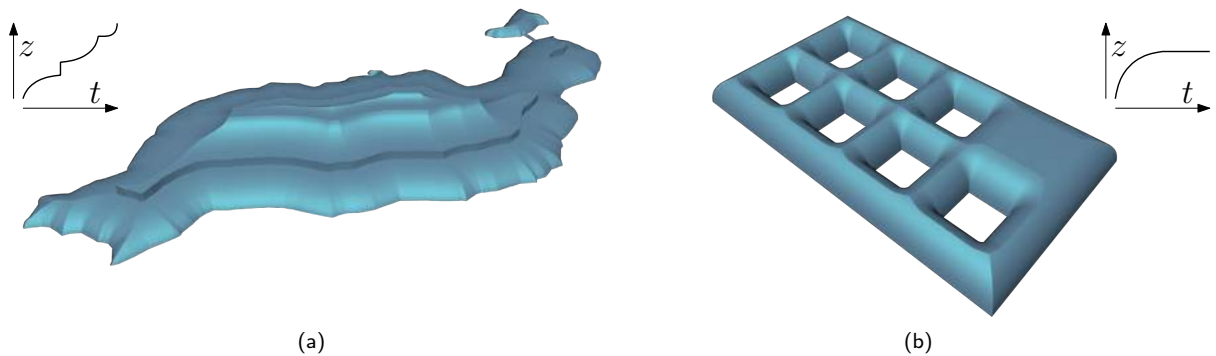


Figure 6: (a) A Voronoi-based chamfered terrain over the outline of Lanzarote, the easternmost of the Spanish Canary Islands in the Atlantic Ocean. (b) The Voronoi-based chamfered surface of a polygon with square holes using the Round-Over chamfer already seen in Figures 4(b) and 4(h). The height functions are illustrated in the corners.

The facets of $\mathcal{T}_f(P)$ can be seen as complex chamfers. For the the standard Voronoi diagram and straight skeleton these chamfers will be symmetric: Locally the two facets on the two sides of a ridge or valley have the same geometry. Asymmetric chamfers can be modeled by resorting to weighted straight skeletons. An additive edge weight causes a facet of $\mathcal{T}_f(P)$ to start at a higher z -level. Multiplicative weights change the “inclination” of a facet by giving it a steeper gradient or making it inclined more gently. We refer to [13] for a discussion of the use of additive and multiplicative weights for the generation of roofs and terrains.

Of course, we can apply our approach also to additively and multiplicatively weighted straight skeletons, thus providing a genuine extension of the roofs presented in [13]. A sample combination of a multiplicatively weighted straight skeleton with a height function f is shown Figure 5(b). (The left, front, and right edges of P have multiplicative weights 4, 1, and $1/2$, respectively.)

5 IMPLEMENTATIONAL ISSUES

We have developed a proof-of-concept code to construct complex chamfers (and fillets) based on our terrains. The construction process runs in two stages. In the first stage we use our existing codes `Vroni`/`ARCVroni` [10, 12] and `Surfer` [15] to generate a Voronoi diagram or a straight skeleton. In our current implementation, conic edges of the Voronoi diagram get sampled and approximated by short straight-line segments. As a result we get a list of polygonal faces, where every face is encoded by a circular list of vertices. Faces in a Voronoi diagram which stem from reflex vertices are triangulated as a triangle fan hinged at the reflex vertex. In addition to the x - and y -coordinates we store with every vertex its appropriate distance t . That is, every vertex can already be seen as a point in three dimensions,

and all 2D faces actually form facets of a roof in 3D. In particular, the standard roof $\mathcal{R}(P)$ would be available without further post-processing, cf. Figures 4(a) and 4(g).

In the second step we obtain a terrain by taking a height function and the standard roof from the previous step. Our current implementation supports cubic B-splines as simple yet powerful and flexible height functions. (Recall that repeating one control point p three times forces the cubic B-spline to pass through p , thus creating a sharp corner at p .) Needless to say, our code could be adapted readily to other height functions.

All facets of the standard roof get split into triangles and trapezoids by a set of t -isocontours. These contours correspond to the intersection of horizontal planes with the standard roofs. The isocontours are not spaced uniformly. Rather, the distance between two consecutive contours is chosen in dependence on the gradient of the height function at that time. Finally, the height function is applied to the time component of each vertex, thus obtaining (x, y, z) -coordinates from (x, y, t) -coordinates. For rendering purposes the output of our second stage is imported into Blender [4].

6 CONCLUSION

We extend our work [13] on skeleton-based roofs over some polygon P by waiving the restriction that the z -coordinate of a point of the roof is given by t if its normal projection onto the xy -plane has the boundary clearance t . By varying the function f that maps t to a z -coordinate $f(t)$ we obtain a large family of terrain-like surfaces over P , for every fixed skeletal structure within P . Natural candidates for such a skeletal structure are the Voronoi diagram and (additively and multiplicatively weighted) straight skeletons of P . As discussed and illustrated by the images provided, it depends on the particular application sought which of the two skeletal structures provides the “better” result. In any case, our approach allows to compute chamfer and fillet surfaces for extruded objects with (polygonal) footprint P efficiently and reliably even in the presence of complex miters. In particular, no all-pairs intersection computations are necessary in order to determine the interactions of the chamfer facets.

ACKNOWLEDGMENTS

This work was supported by Austrian Science Fund (FWF): P25816-N15 and ORD 53-VO.

ORCID

Martin Held  <http://orcid.org/0000-0003-0728-7545>

Peter Palfrader  <http://orcid.org/0000-0002-5796-6362>

REFERENCES

- [1] Aichholzer, O.; Aurenhammer, F.; Alberts, D.; Gärtner, B.: A Novel Type of Skeleton for Polygons. *Journal of Universal Computer Science*, 1(12), 752–761, 1995. http://doi.org/10.1007/978-3-642-80350-5_65.
- [2] Biedl, T.; Held, M.; Huber, S.; Kaaser, D.; Palfrader, P.: A Simple Algorithm for Computing Positively Weighted Straight Skeletons of Monotone Polygons. *Information Processing Letters*, 115(2), 243–247, 2015. <http://doi.org/10.1016/j.ipl.2014.09.021>.
- [3] Biedl, T.; Held, M.; Huber, S.; Kaaser, D.; Palfrader, P.: Weighted Straight Skeletons in the Plane. *Computational Geometry: Theory and Applications*, 48(2), 120–133, 2015. <http://doi.org/10.1016/j.comgeo.2014.08.006>.
- [4] Blender: Free and Open Source Graphics Software. <https://www.blender.org/>.
- [5] Blum, H.: A Transformation for Extracting New Descriptors of Shape. In *Models for the Perception of Speech and Visual Form*, 362–380. MIT Press, Cambridge, MA, USA, 1967.
- [6] Chin, F.; Snoeyink, J.; Wang, C.: Finding the Medial Axis of a Simple Polygon in Linear Time. *Discrete & Computational Geometry*, 21(3), 405–420, 1999.
- [7] Eppstein, D.; Erickson, J.: Raising Roofs, Crashing Cycles, and Playing Pool: Applications of a Data Structure for Finding Pairwise Interactions. *Discrete & Computational Geometry*, 22(4), 569–592, 1999. <http://doi.org/10.1145/276884.276891>.
- [8] Fortune, S.: A Sweepline Algorithm for Voronoi Diagrams. *Algorithmica*, 2(2), 153–174, 1987.

- [9] Held, M.: Roofs, Terrains, Chamfers and Fillets Based on Skeletal Structures. <https://www.cosy.sbg.ac.at/~held/projects/roofs/roofs.html>.
- [10] Held, M.: VRONI: An Engineering Approach to the Reliable and Efficient Computation of Voronoi Diagrams of Points and Line Segments. *Computational Geometry: Theory and Applications*, 18(2), 95–123, 2001. [http://doi.org/10.1016/S0925-7721\(01\)00003-7](http://doi.org/10.1016/S0925-7721(01)00003-7).
- [11] Held, M.: VRONI and ArcVRONI: Software for and Applications of Voronoi Diagrams in Science and Engineering. In 8th International Symposium on Voronoi Diagrams in Science and Engineering (ISVD), 3–12, 2011. <http://doi.org/10.1109/ISVD.2011.9>.
- [12] Held, M.; Huber, S.: Topology-Oriented Incremental Computation of Voronoi Diagrams of Circular Arcs and Straight-Line Segments. *Computer-Aided Design*, 41(5), 327–338, 2009. <http://doi.org/10.1016/j.cad.2008.08.004>.
- [13] Held, M.; Palfrader, P.: Straight Skeletons with Additive and Multiplicative Weights and Their Application to the Algorithmic Generation of Roofs and Terrains. *Computer-Aided Design*, 92, 33–41, 2017. <http://doi.org/10.1016/j.cad.2017.07.003>.
- [14] Huber, S.; Held, M.: A Fast Straight-Skeleton Algorithm Based On Generalized Motorcycle Graphs. *International Journal of Computational Geometry & Applications*, 22(5), 471–498, 2012. <http://doi.org/10.1142/S0218195912500124>.
- [15] Palfrader, P.; Held, M.; Huber, S.: On Computing Straight Skeletons by Means of Kinetic Triangulations. In 20th Annual European Symposium on Algorithms (ESA), vol. 7501 of Lecture Notes in Computer Science, 766–777. Springer-Verlag, 2012. http://doi.org/10.1007/978-3-642-33090-2_66.
- [16] Peschka, G.A.v.: *Kotirte Projektionsmethode (Kotirte Ebenen) und deren Anwendung*. Buschak & Irrgang, Brünn, 1882.
- [17] Tănase, M.; Veltkamp, R.C.: A Straight Skeleton Approximating the Medial Axis. In 12th Annual European Symposium on Algorithms (ESA), vol. 3221 of Lecture Notes in Computer Science, 809–821. Springer-Verlag, 2004. http://doi.org/10.1007/978-3-540-30140-0_71.
- [18] Vigneron, A.; Yan, L.: A Faster Algorithm for Computing Motorcycle Graphs. In 29th Symposium on Computational Geometry (SoCG), 17–26. Rio de Janeiro, Brazil, 2013. <http://doi.org/10.1145/2462356.2462396>.
- [19] Yap, C.: An $O(n \log n)$ Algorithm for the Voronoi Diagram of a Set of Simple Curve Segments. *Discrete & Computational Geometry*, 2(4), 365–393, 1987.